**Supporting Information**

# Mixed Phase 2D $MoWS_2$ Alloy as Multi-Functional Electrocatalyst for the High-Performance Cathode in Li-S Batteries

Sanket Bhoyate[a1], Junyoung Kim[a1], Eunho Lee[b], Bumsu Park[c], Eunji Lee[c], Juhong Park[a], Sang Ho Oh[c], Jeongyong Kim[c], Wonbong Choi[a,b*]

[a] Department of Materials Science and Engineering, University of North Texas, Denton, Texas 76203, United States

[b] Department of Mechanical and Energy Engineering, University of North Texas, Denton, Texas 76203, United States

[c] Department of Energy Science, Sungkyunkwan University, Suwon 16419, Republic of Korea

**Keywords**: $MoWS_2$, 2D alloy, Lithium polysulfide, Catalysts, Li-S battery

***Corresponding author**: wonbong.choi@unt.edu

| | Molybdenum | Tungsten | Sulfur | Ratio |
|---|---|---|---|---|
| **$MoS_2$** | 32.47 | - | 67.53 | 1:2 |
| **$WS_2$** | - | 33.62 | 66.38 | 1:2 |
| **$MoWS_2$** | 16.70 | 15.89 | 67.41 | 1:1:4 |

**Table 1.** Atomic concentration and the ratio of each catalyst, $MoS_2$, $WS_{2,}$ and $MoWS_{2,}$ on CNT paper, analyzed using XPS data.

| 2D Catalyst-Cathode | Initial capacity (mAh/g) / C-rate used | Capacity after 100th cycle (mAh/g) | Reference |
|---|---|---|---|
| ***$Mo_{0.5}W_{0.5}S_2$-CNT-S*** | ***1001 (0.5C)*** | ***934*** | ***This work*** |
| ***$MoS_2$-CNT-S*** | ***802 (0.5C)*** | ***680*** | ***This work*** |
| ***$WS_2$-CNT-S*** | ***679 (0.5C)*** | ***675*** | ***This work*** |
| $MoS_2$/RGO/S | ~900 (0.5C) | ~720 | [1] |
| $MoS_2$@N-doped carbon interlayer | 1095 (0.5C) | 880 | [2] |
| $MoS_{2-x}$/rGO/S | 1159.9 (0.5C) | ~819.9 | [3] |
| $MoS_2$/CNTP | 1233 (0.5C) | ~850 | [4] |
| $MoS_2$-coated N-doped mesoporous carbon sphere/sulfur | ~900 (0.5C) | ~600 | [5] |
| Cage-like $MoS_2$ | ~600 (0.5C) | ~590 | [6] |
| Vertically aligned $MoS_2$ | ~900 (0.5C) | ~1000 | [6] |
| MXene/1T-2H $MoS_2$-C-S | 1014 (0.5C) | 799.3 | [7] |
| Defect-Rich $MoS_2$ Nanosheets | 1429 (0.2C) | 821 | [8] |
| 3D-Graphene/2H-$MoS_2$ | ~1000 (0.1C) | ~726 | [9] |
| 3D-Graphene/1T-$MoS_2$ | 1181 (0.1C) | ~1133 | [9] |
| $MoS_2$/S/rGO | ~1000 (2C) | ~750 | [10] |
| $MoS_3$/rGO | 1000 (2C) | ~850 | [11] |
| $WS_2$-rGO-CNT | 1100 (0.5C) | 860 | [12] |

**Table 2.** Comparison of $Mo_{0.5}W_{0.5}S_2$ alloy with recently reported 2D materials as LiPSs catalysts for Li-S battery.

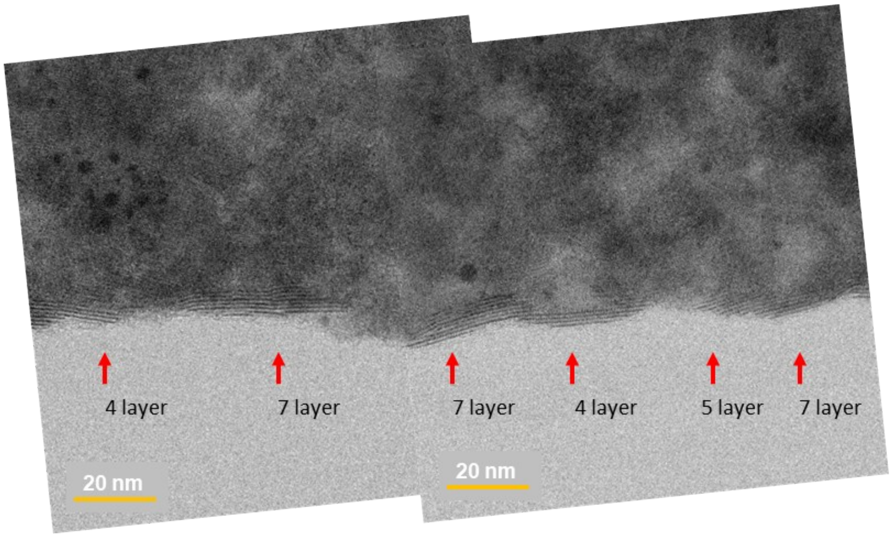


**Fig. S1** HRTEM image of 4 to 7 layer 2D $Mo_{0.5}W_{0.5}S_2$ alloy deposited on a carbon TEM grid. An average thickness of $Mo_{0.5}W_{0.5}S_2$ was 8 nm, with polycrystalline grain sizing from 20 to 50 nm.

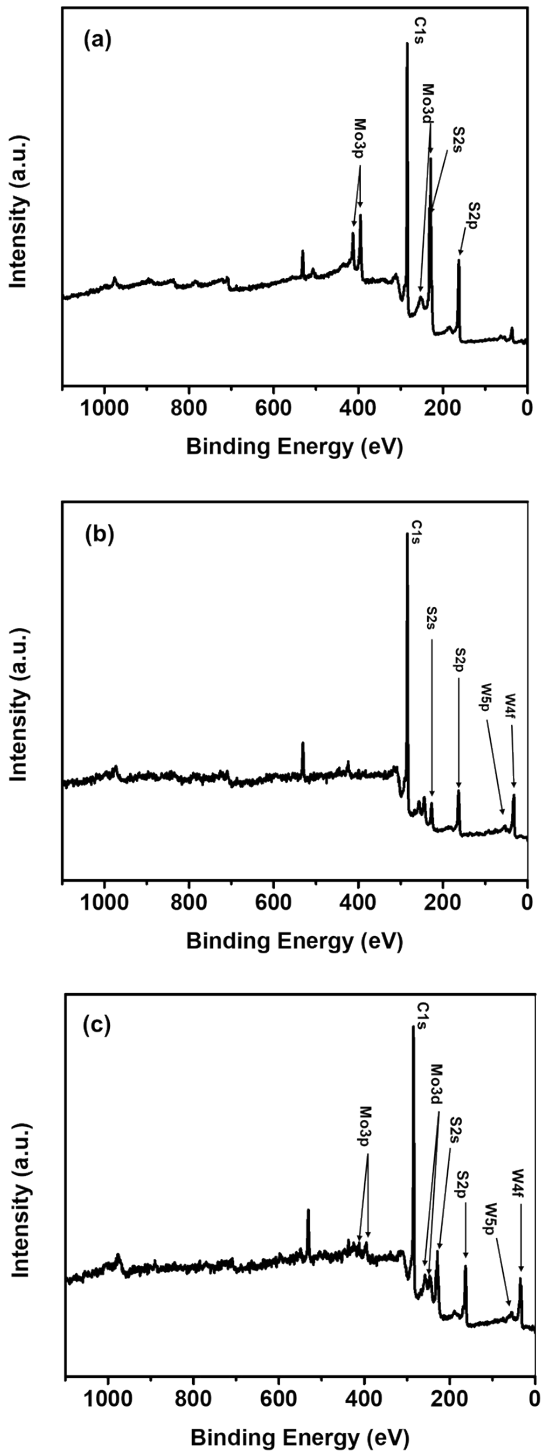


**Fig. S2** Survey form X-ray photoelectron spectroscopy (XPS) analysis of (a) $MoS_2$, (b) $WS_2$, and (c) $Mo_{0.5}W_{0.5}S_2$ catalyst coated on CNT paper.

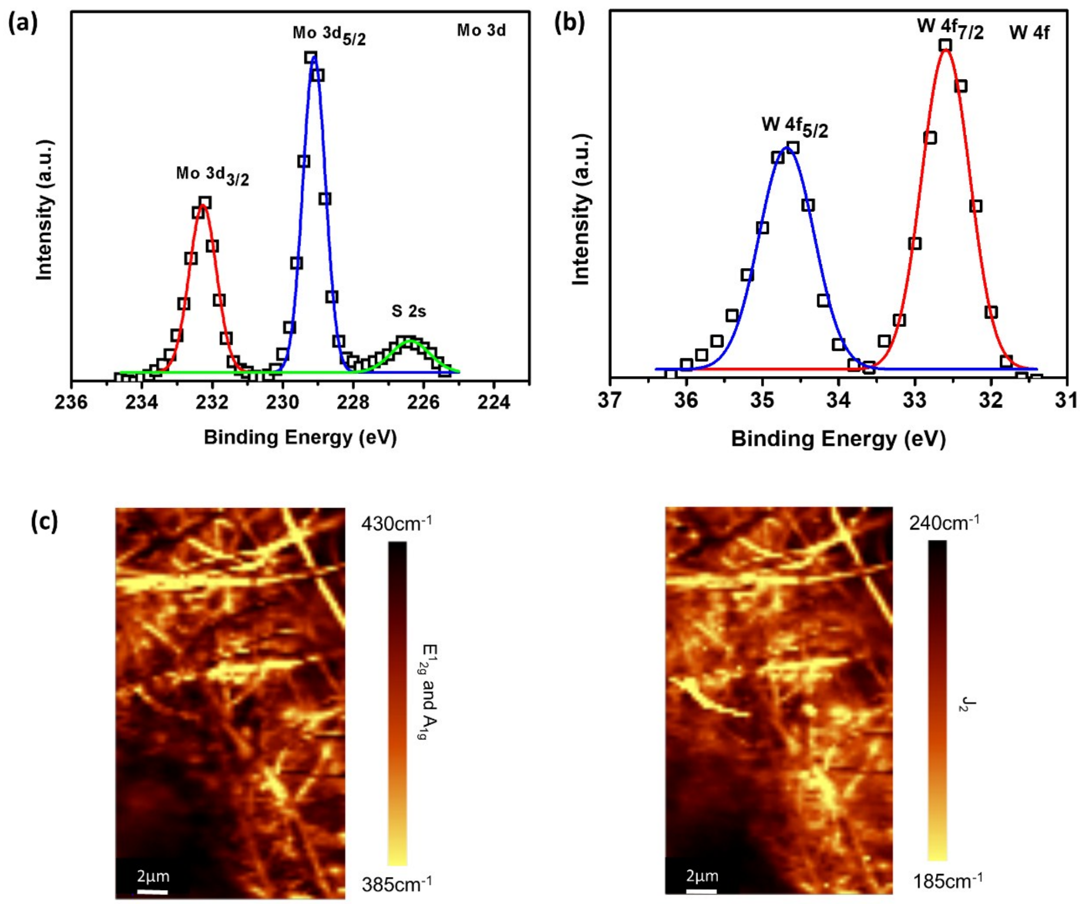


**Fig. S3** X-ray photoelectron spectroscopy (XPS) analysis of (a) $MoS_2$ and (b) $WS_2$ catalyst coated on CNT paper. (c) $E^1_{2g}/A_{1g}$ and $J_2$ Raman mapping for $Mo_{0.5}W_{0.5}S_2$ coated on CNT paper.

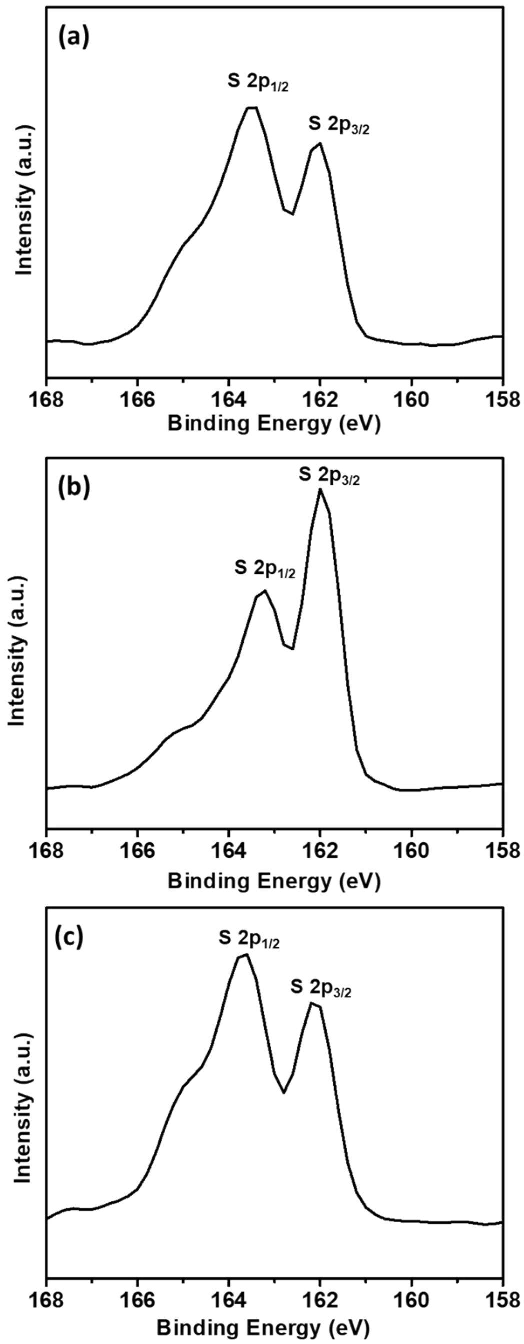


**Fig. S4** S 2p spectra from XPS for (a) $Mo_{0.5}W_{0.5}S_2$, (b) $MoS_2$ and, (c) $WS_2$ on CNT paper used for fabricating Li-S battery.

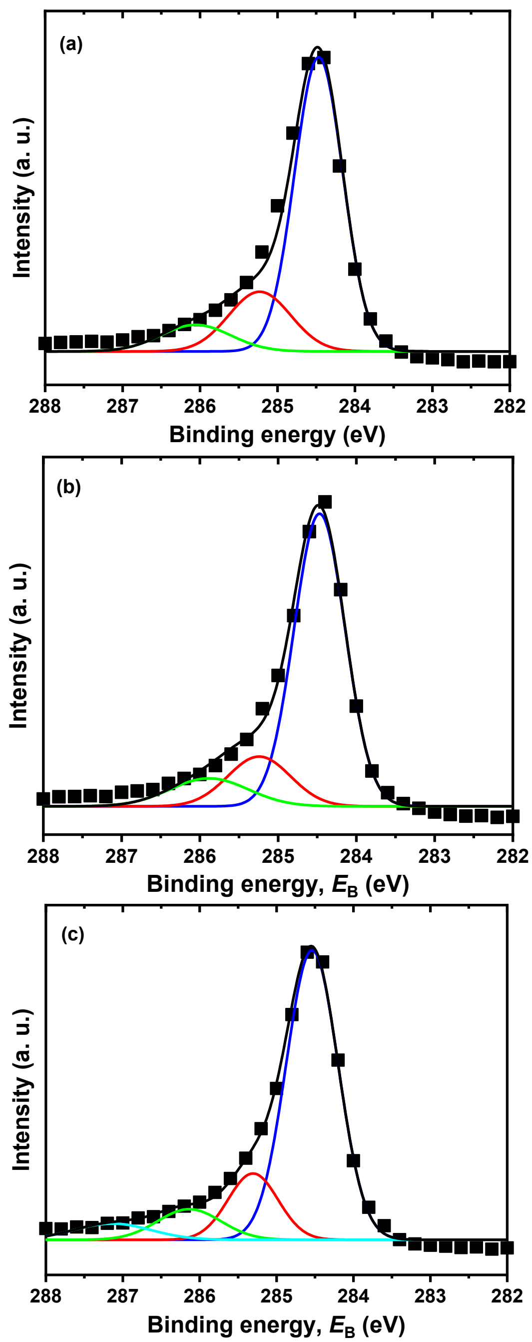


**Fig. S5** C 1s spectra from XPS for (a) $MoS_2$, (b) $WS_2$ and, (c) $Mo_{0.5}W_{0.5}S_2$ on CNT paper used for fabricating Li-S battery. The spectra show the bonding behavior of catalysts on CNT paper (C-S bond near 285.36 eV). The bonding formation results in an electronic couple and stable structure, allowing ease in electron transfer between the catalyst and CNT paper during the charging and discharging cycles of the Li-S battery.

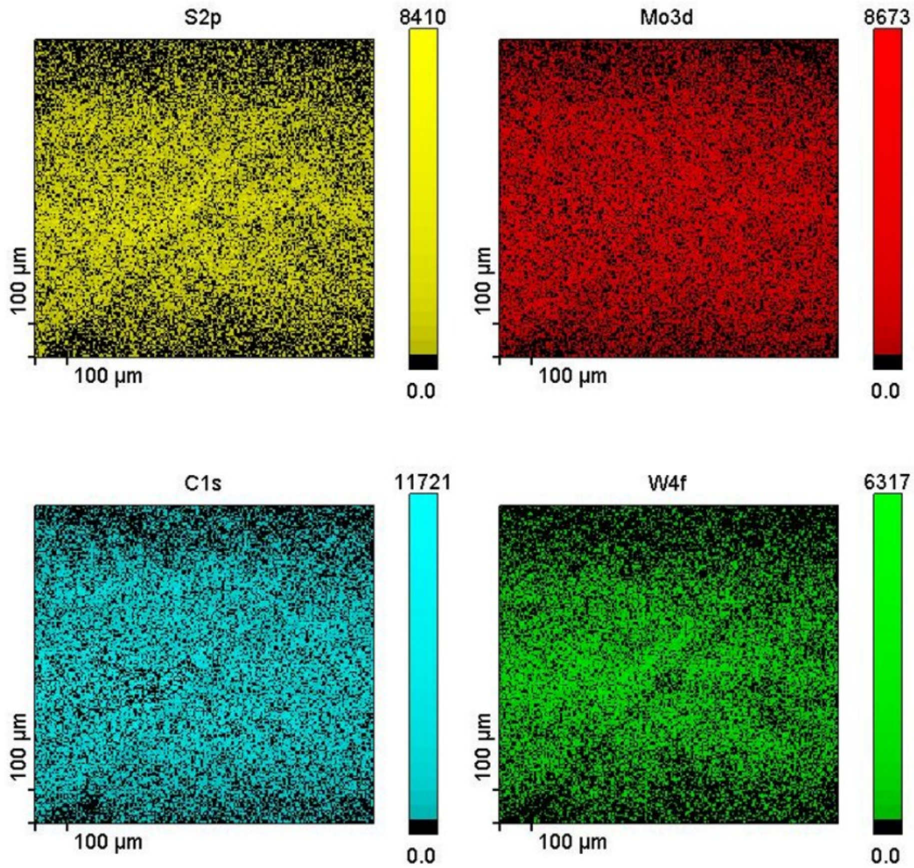


**Fig. S6** Large area XPS-EDX elemental mapping of sulfur, molybdenum, carbon, and tungsten in 2D $Mo_{0.5}W_{0.5}S_2$ catalyst deposited on CNT paper. The spectra suggest uniform dispersion of all the elements coated on CNT paper.

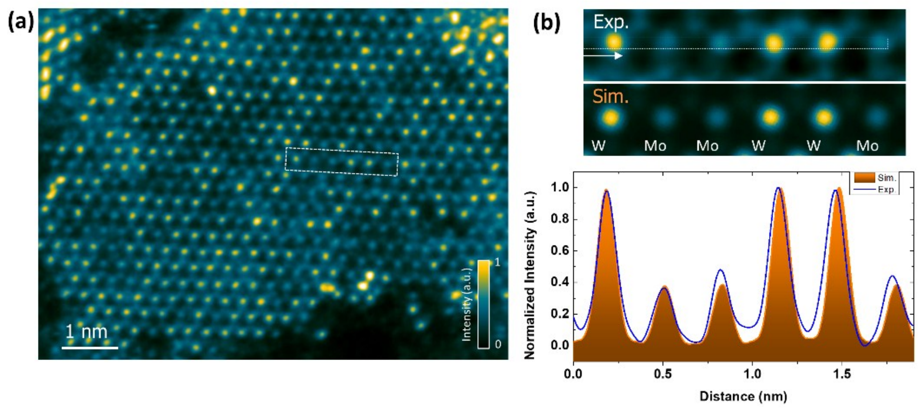


**Fig. S7** (a) High magnification HAADF-STEM image with (b) an intensity profile of atoms showing Mo and W are uniformly distributed by sharing an adjacent S atom.

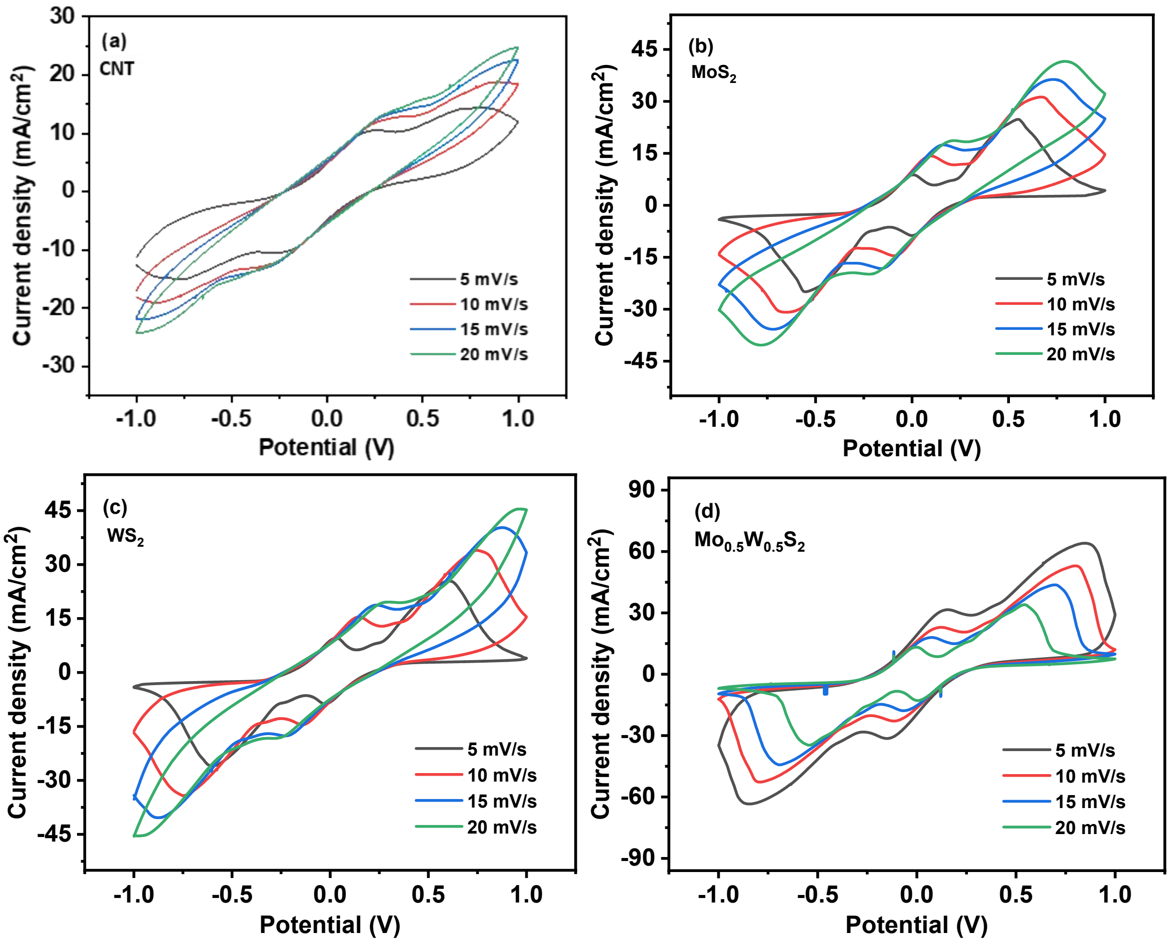


**Fig. S8** CV curves for symmetrical cell test for all the cathodes in 50 µL of 0.2M $Li_2S_6$/1M LiTFSI solution. The data suggest oxidation-reduction behavior during the electrochemical conversion of LiPSs from elemental sulfur and back to LiPSs. The 2D $Mo_{0.5}W_{0.5}S_2$ coated CNT paper showed higher redox peak intensity suggesting improved LiPSs conversion.

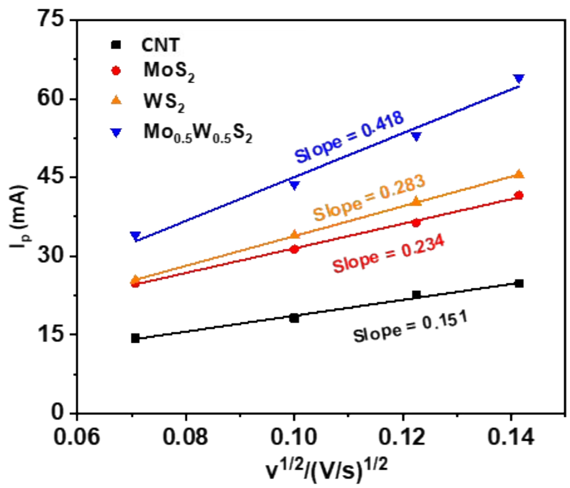


**Fig. S9** The calculated slope by plotting peak current ($I_p$) versus square root of scan rate $(V/s)^{1/2}$. Higher slope values suggest faster diffusion of Li-ions through the 2D $Mo_{0.5}W_{0.5}S_2$ coated CNT-S cathode.

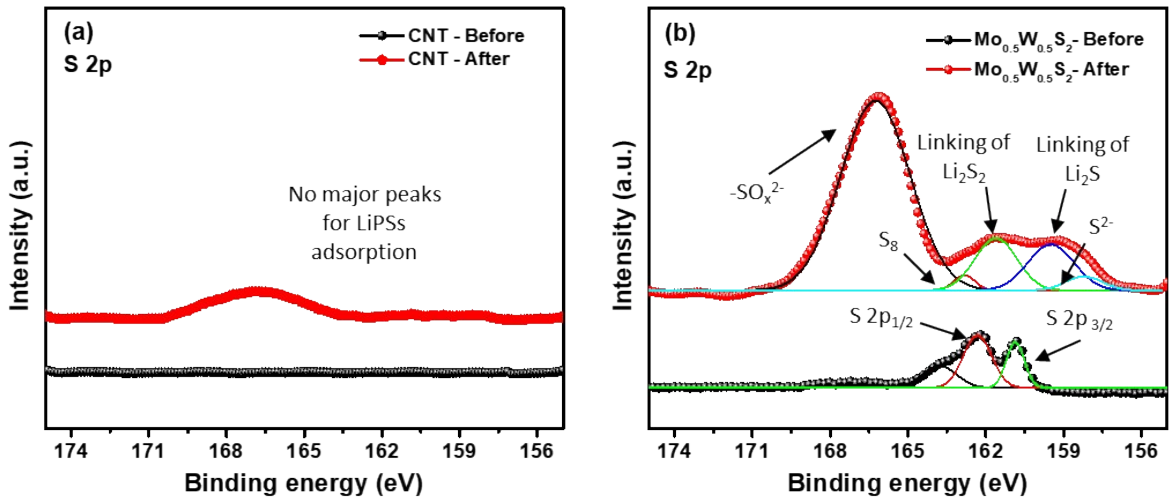


**Fig. S10** XPS analysis of (a) Bare-CNT-paper and (b) $Mo_{0.5}W_{0.5}S_2$-CNT paper before and after polysulfide absorption test in 2 mmol $Li_2S_6$ solutions for 10 h. The S 2p peaks for $Mo_{0.5}W_{0.5}S_2$ (S $2p_{1/2}$ and S $2p_{3/2}$) broaden and shift towards lower binding energy suggesting adsorption of LiPSs on the $Mo_{0.5}W_{0.5}S_2$ catalyst surface after polysulfide adsorption test was performed.[13]

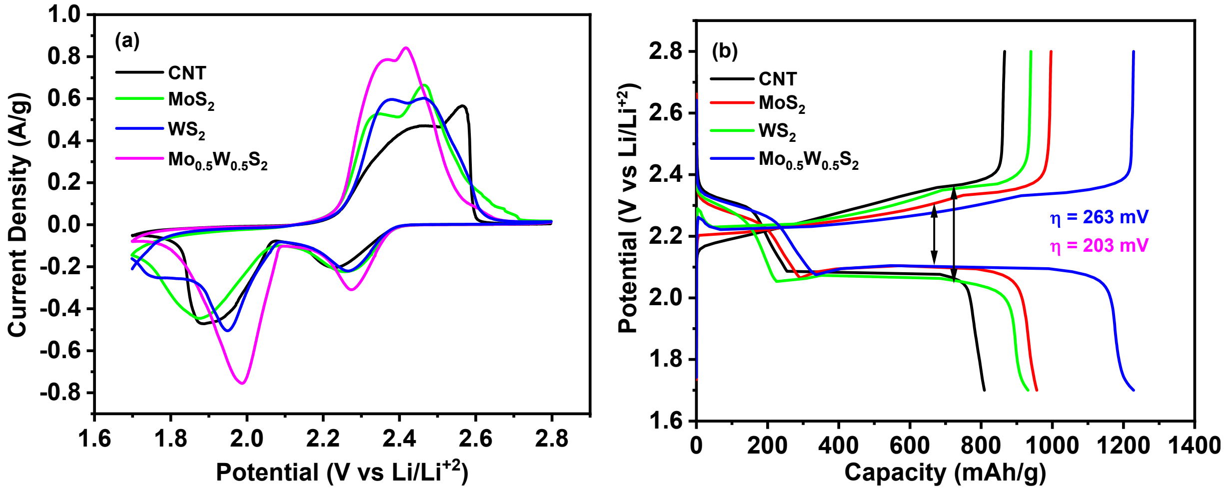


**Fig. S11** (a) CV curves and, (b) Galvanostatic curves at 0.1C for $MoS_2$, $WS_2$, and $Mo_{0.5}W_{0.5}S_2$ coated cathodes using full cell Li-S battery. The CV curves show the systematic shift of redox peaks and increase in peak intensities suggesting improved LiPSs conversion. This behavior results in a higher discharge capacity of the final Li-S battery.

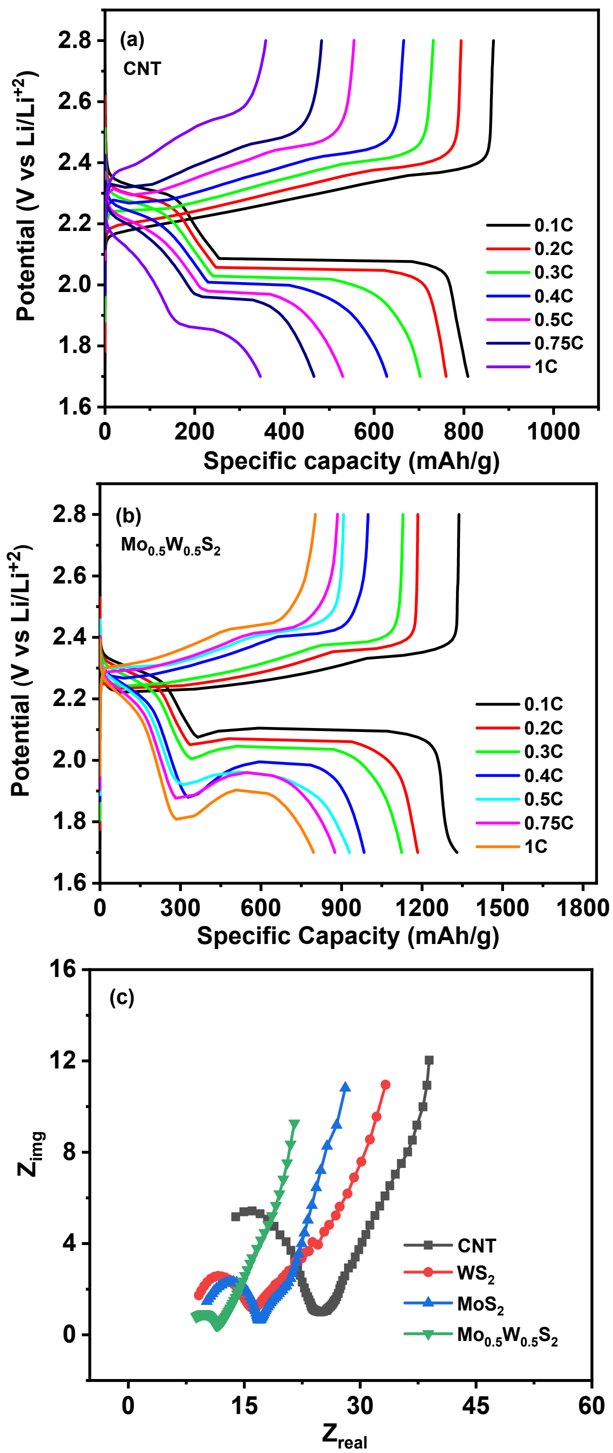


**Fig. S12** Galvanostatic curves for (a) bare and (b) $Mo_{0.5}W_{0.5}S_2$ coated CNT paper cathodes characterized in full cell Li-S battery at different C-rates. (c) Nyquist plot for bare CNT-sulfur and 2D TMD catalyst coated CNT-sulfur cathodes.

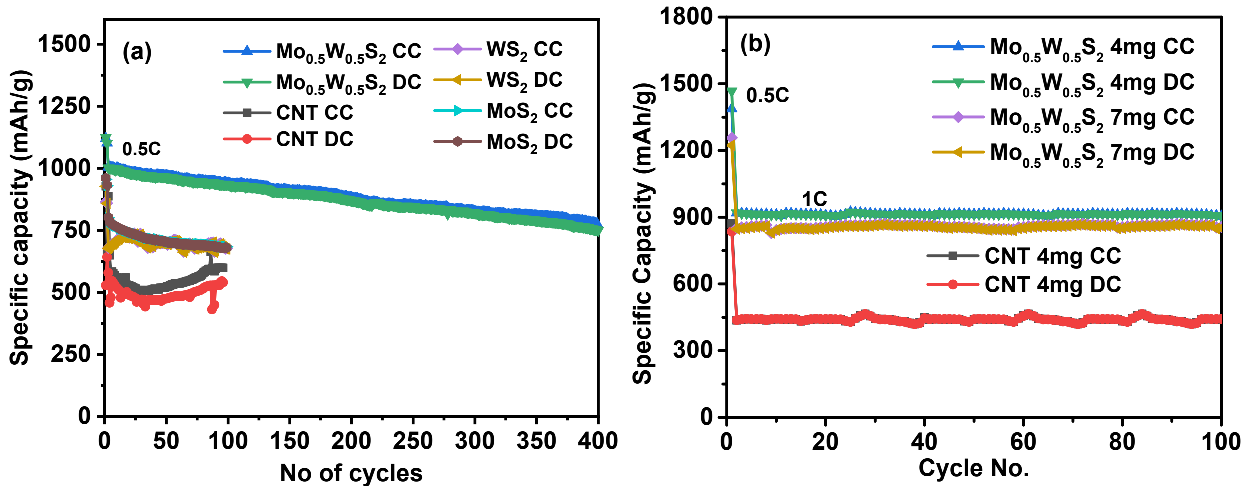


**Fig. S13** Stability plots for Li-S full cells using $MoS_2$, $WS_2$, and $Mo_{0.5}W_{0.5}S_2$ catalyst coated CNT cathode (CC = charge capacity and DC = discharge capacity). (a) Cyclic stability at 0.5C. (b) Cyclic stability at 1C with various sulfur loadings. The 2D $Mo_{0.5}W_{0.5}S_2$ catalyst coated CNT cathode retained a high specific capacity even at high sulfur loading of 7 mg/cm$^2$.

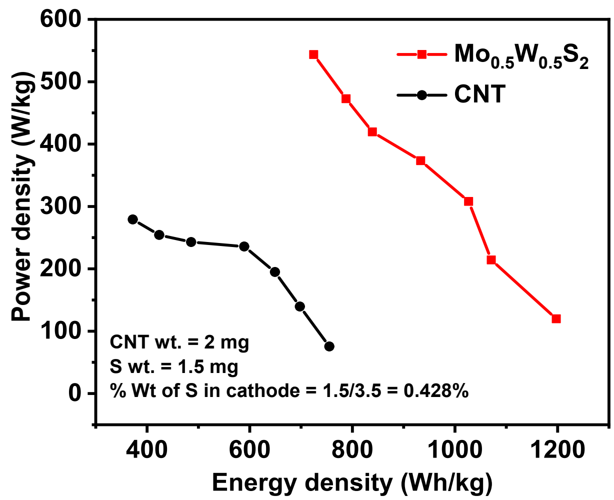


**Fig. S14** Ragone plot for Li-S full cells fabricated using the bare CNT and 2D $Mo_{0.5}W_{0.5}S_2$ catalyst coated on CNT paper as a sulfur cathode. The calculations have been performed using a complete weight of cathode (CNT paper + S cathode).

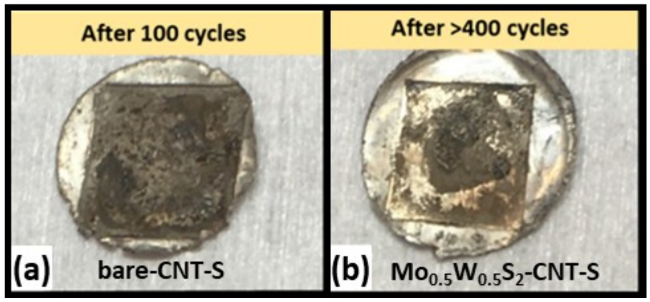


**Fig. S15** Images of disassembled Li-anode after cycling test in coin cells. (a) The Li-anode without a catalyst coated on CNT-S cathode was quite brittle, especially near the portions of intense corrosion after the cycling. (b) There was no such behavior observed in Li-anode when it was assembled with a 2D $Mo_{0.5}W_{0.5}S_2$ catalyst coated CNT-S cathode.

**Calculations for Li-ion diffusion coefficients:**

$$I_p = 2.69 \times 10^5 n^{1.5} A D_{Li+}^{0.5} C v^{0.5} C_{Li}$$

n = no of electrons = 2

A = area = 1 $cm^2$

$C_{Li}$ = Li-ion concentration change in reaction = 0.001 mol/$cm^3$

V = scan rate (mV/s)

$D_{Li+}$ = Li ion diffusion coefficient

To simplify,

$$D_{Li+} = [I_p / 2.69 \times 10^5 n^{1.5} A\, C v^{0.5} C_{Li}]^2$$

For, i) Bare CNT = $I_p/v^{0.5}$ = 0.151

ii) $MoS_2$ = 0.234

iii) $WS_2$ = 0.283

iv) $Mo_{0.5}W_{0.5}S_2$ = 0.418

The calculated Li-ion diffusion coefficients were $D_{Li+}^{Bare\ CNT}$ = 1.5 x $10^{-9}$ $cm^2$/s, $D_{Li+}^{MoS2}$ = 3.78 x $10^{-9}$ $cm^2$/s, $D_{Li+}^{WS2}$ = 5.5 x $10^{-9}$ $cm^2$/s and $D_{Li+}^{Mo0.5W0.5S2}$ = 1.2 x $10^{-8}$ $cm^2$/s.

## References


1 Y. You, Y. Ye, M. Wei, W. Sun, Q. Tang, J. Zhang, X. Chen, H. Li and J. Xu, *Chem. Eng. J.*, 2019, **355**, 671.

2 J. Wu, X. Li, H. Zeng, Y. Xue, F. Chen, Z. Xue, Y. Ye and X. Xie, *J. Mater. Chem. A*, 2019, **7**, 7897.

3 H. Lin, L. Yang, X. Jiang, G. Li, T. Zhang, Q. Yao, G. W. Zheng and J. Y. Lee, *Energy Environ. Sci.*, 2017, **10**, 1476.

4 J. Li, Y. Jiang, F. Qin, J. Fang, K. Zhang and Y. Lai, *J. Electroanal. Chem.*, 2018, **823**, 537.

5 S. Jiang, M. Chen, X. Wang, Z. Wu, P. Zeng, C. Huang and Y. Wang, *ACS Sustain. Chem. Eng.*, 2018, **6**, 16828.

6 H. T. Wang, Q. F. Zhang, H. B. Yao, Z. Liang, H. W. Lee, P. C. Hsu, G. Y. Zheng and Y. Cui, *Nano Lett.*, 2014, **14**, 7138.

7 Y. Zhang, Z. Mu, C. Yang, Z. Xu, S. Zhang, X. Zhang, Y. Li, J. Lai, Z. Sun, Y. Yang, Y. Chao, C. Li, X. Ge, W. Yang and S. Guo, *Adv. Funct. Mater.*, 2018, **28**, 1707578.

8 M. Liu, C. Zhang, J. Su, X. Chen, T. Ma, T. Huang and A. Yu, *ACS Appl. Mater. Interfaces*, 2019, **11**, 20788.

9 J. He, G. Hartmann, M. Lee, G. S. Hwang, Y. Chen and A. Manthiram, *Energy Environ. Sci.*, 2019, **12**, 344.

10 Y. Wei, Z. Kong, Y. Pan, Y. Cao, D. Long, J. Wang, W. Qiao and L. Ling, *J. Mater. Chem. A*, 2018, **6**, 5899.

11 A. Mammoottil Abraham, S. P. Kammampata, S. Ponnurangam and V. Thangadurai, *ACS Appl. Mater. Interfaces*, 2019, **11**, 35729.

12 S. Huang, Y. Wang, J. Hu, Y. Von Lim, D. Kong, Y. Zheng, M. Ding, M. E. Pam and H. Y. Yang, *ACS Nano*, 2018, **12**, 9504.

13 H. Lin, L. Yang, X. Jiang, G. Li, T. Zhang, Q. Yao, G. W. Zheng and J. Y. Lee, *Energy Environ. Sci.*, 2017, **10**, 1476.